Original Paper

Eletrônica de Potência
Open Journal of Power Electronics

Received July 26, 2024; accepted October 02, 2024; Date of publication October 14, 2024.
The review of this paper was arranged by Associate Editor Allan F. Cupertino and Editor-in-Chief Heverton A. Pereira.
Digital Object Identifier http://doi.org/10.18618/REP.e202439

Harmonics Measurement Errors in Grids with High Presence of Power Electronics Converters

Gustavo Ortenzi[1], Emmanuel Sangoi[2], José A. Pomilio[1], João I. Y. Ota[1], Rafael K. Carneiro[1]

[1]Universidade Estadual de Campinas, Departamento de Sistemas e Energia, Campinas, Brasil.
[2]National Technological University, Santa Fe, Argentina.

e-mail: g037363@dac.unicamp.br, esangoi@frsf.utn.edu.ar, antenor@unicamp.br, joao.inacio.ota@gmail.com, rafael.k.carneiro@gmail.com

ABSTRACT The article presents field results and discusses the harmonic measurement errors of power quality analyzers (PQA) due to sampling aliasing of currents and voltages in grids with the presence of power electronics converters (PEC). The PQA may imply non-existing harmonic components incorrectly depending on the sampling rate of the PQA and the switching frequency of the PEC. Such phenomenon is prone to become more common and unpredictable due to the amplification of high-frequency components in voltages and currents due to interactions between PEC, loads, and grid elements. The conclusion is that PQAs, as required by standards in use currently, are not prepared to identify and quantify, when necessary and correctly, the high-frequency components that are present in modern electric networks with multiple PECs.

KEYWORDS Microgrids, Power Quality, Power Quality Analyzer, Smart Grids, Supra Harmonics.

I. INTRODUCTION

Electric power quality (PQ) standards have been deliberated carefully and updated frequently to inform reliable measurement criteria provided by a PQ analyzer (PQA). The EN 61000-4-30 [1] consolidates procedures from distinct standards used to assess specific PQ disturbances and is the reference for the specification of PQAs. Nevertheless, technological advances may require revisions in standards if neither normative foresight nor a proper measurement method exists for unexpected phenomena.

The EN 61000-4-30 defines two classes of instruments:

• Class A: used for precise measurements, such as contractual applications resolving disputes, verifying compliance with standards, etc.

• Class S: used for statistical applications such as surveys or power quality assessment, possibly with a limited subset of parameters. Although using measurement intervals equivalent to Class A, the Class S processing requirements are much lower.

The dissemination of microgrids [2] and the extensive use of distributed energy resources (DERs) associated with power electronics converters (PECs) pose an important ongoing paradigm shift in the electrical grid. The IEEE 1547 [3] is a standard for connecting DER systems to the grid. It defines how solar, wind, storage, and other inverter-based DERs must be connected to the grid. This standard defines conformance testing and requires that IEC 61000-4-30 Class A compliant PQ meters are used for voltage & current distortion and other evaluations.

An issue under discussion is the unknown effect of the pulse width modulation (PWM) switching frequency of PECs on modern grids. While the PWM frequency of PECs is typically 10-100 kHz depending on the PEC power, PQ standards state the limits of current and voltage distortion in a frequency range of 50-2000 Hz or 60-3000 Hz [4]. Note that the conductive distortion limits above 150 kHz are well established by standards related to electromagnetic interference (EMI), such as the IEC-CISPR standards [5].

Although considered an isolated and harmless phenomenon until recently, the frequency range of 3-150 kHz distortion in the grid has been reported as a potential EMI risk [6] and a PQ issue [7-10]. Note that multiple PECs may amplify such distortions due to the potential resonance among the filters of the PECs [10]. Power system researchers labeled the frequency range of 3-150 kHz as “supra harmonics” [11-13] to highlight the concerns about the still unclear effects.

This scenario is typical of microgrids due to the inherently large presence of converters. Still, it is also increasingly common in conventional grids with the proliferation of PV systems and, more recently, electric vehicle chargers, in addition to other power converters.

Given the frequency range of the phenomena, they do not propagate beyond the limits of the low-voltage network. They are certainly verifiable within consumer units (CU) [14]. In such a situation, supra harmonics may affect local loads, but it is not characterized as a power quality problem under the responsibility of the power distribution company. However, these phenomena may be observed under certain conditions in the network external to the CUs, circulating between power converters at different network points. In this case, the phenomena could be considered as being under the responsibility or management of the company.

The point focused on in this article is how the main instrument for measuring the conditions of an electrical network, the PQA, operates with a significant presence of disturbances in the "supra harmonic" frequency range.

PQAs use embedded digital systems and digital signal processing. The specification of digital sampling procedures defines the range of harmonics detection of the PQA. However, the sampling is decided mainly to satisfy the existing standards.

When the sampling rate and any spectral component of the signal to be analyzed are at relatively close frequencies, the calculation and analysis algorithms can present incorrect results and may lead to wrong conclusions about the quality of the electric power or the functioning of specific equipment.

The paper is organized as follows: Section II describes how the electric grid, full of PECs, can present substantial high-frequency spectral components due to the interactions among the input stage of these converters; Section III discusses the operational characteristics of the PQAs and how they behave if the electrical signal presents high-frequency components; Section IV presents field measurements taken by distinct Class A PQAs in a low-voltage microgrid with an extensive presence of PECs. A comparison of the measurements is discussed, and it is shown that the aliasing effect led to wrong measurements of harmonics in one of the PQAs, which may lead to misleading interpretations of PQ analysis; Section V presents the conclusions.

II. AMPLIFICATION OF HIGH-FREQUENCY CURRENT IN MODERN GRIDS

First, let us verify how supra harmonic may appear in the current and voltage. The PEC output filters, usually low-pass, second-order LC, are designed to mitigate the propagation of the switching frequency from the PEC to the grid. The design procedure considers the converter connected to a grid with an inductive impedance [15].

Besides the output filter, commercial PECs include an EMI filter between the LC power filter and the PCC. As seen from the grid, the front-end device is a capacitor. The capacitance value depends on the PEC power but is typically in the range of nano to micro-farads.

In an installation with multiple PECs, the grid configuration and the nature of the loads may allow the circulation of high-frequency current among the passive elements of the PEC filters.

This current can achieve significant values, which may affect the grid voltage [7-10]. In particular situations, resonance may occur depending on the distance between the converters (determining the path inductance) and the front-end capacitor, amplifying the switching frequency signals even more. Figure 1 shows the experimental waveforms of two photovoltaic (PV) inverters at different grid nodes.

The PWM switching frequencies of PEC1 and PEC2 are 20 and 19.4 kHz, respectively, as identified in Figure 2. The high-frequency components in the currents are amplified due to the interaction of the passive filters. A 600 Hz beat is noticeable in the currents of both PV inverters, which is explained in [7].

Note that this amplified current is highly dependent on the grid configuration and on the filter of the PECs. Thus, it is rather difficult to predict and prevent its occurrence.

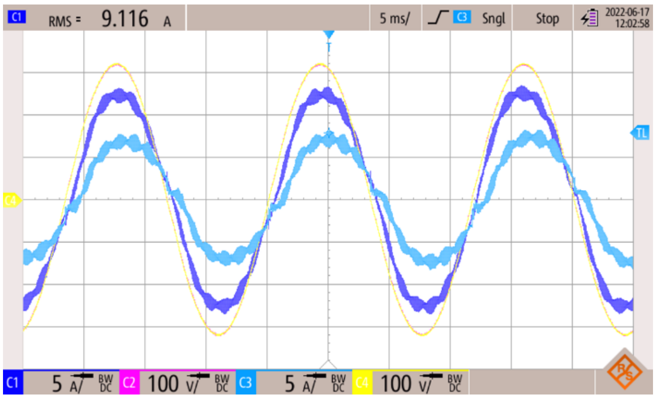

FIGURE 1. Experimental waveforms showing the effect of frequency beat between PECs with amplification of current circulation. Voltage at the point of common coupling (yellow, C4), PEC1 current (dark blue, C1), PEC2 current (blue, C3).

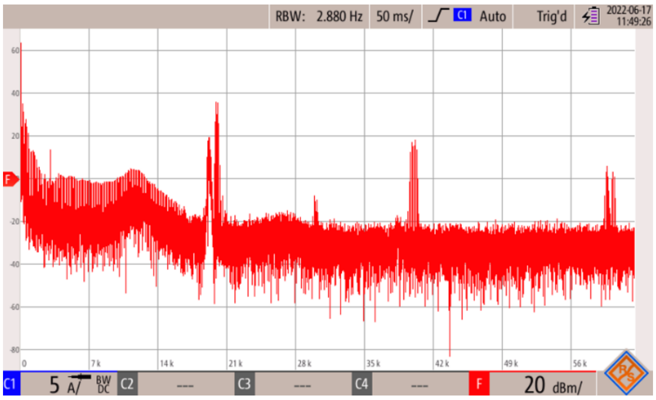

FIGURE 2. The experimental frequency spectrum of PEC1 current, 7 kHz/div.

Figure 3 shows experimental waveforms when a PV inverter injects power into a microgrid (operating in the connected mode), and an equivalent front-end capacitance of 2.2 µF (representing a set of electronic loads) is connected about 25 m far from the PV inverter PCC. This capacitance and the equivalent wiring inductance induce a resonance with the inverter's 20-kHz switching frequency. At the load PCC, the high-frequency component of current and voltage reaches more than 5 A peak-to-peak and 18 V peak-to-peak, respectively.

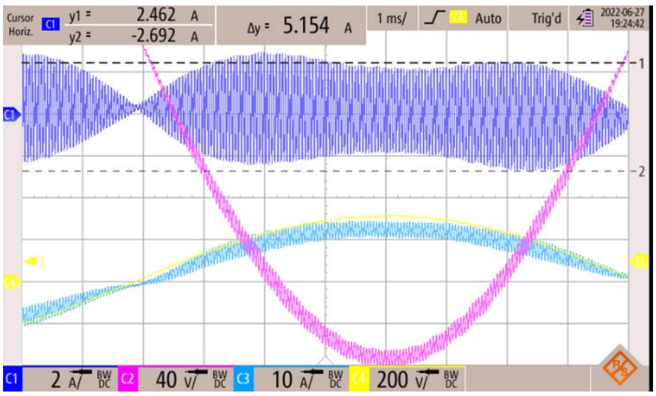

FIGURE 3. Experimental waveforms showing the interaction between PV inverter and capacitive load (2.2 uF) distanced by 25 m. Current (dark blue, C1) and detail of the voltage (magenta, C2) on the load. PV inverter current (blue, C3) and voltage (yellow, C4).

The PV PEC used in this experiment has a 500 V DC bus. Despite not knowing the exact inverter filtering characteristics, the design procedures usually provide at least a 40 dB attenuation at the switching frequency. Considering an LC filter, this shall result in a residual voltage of a few Volts on the filter capacitor. This small voltage is enough to excite the resonance formed by the feeder cable inductance and load equivalent capacitance, amplifying the voltage and current at this specific frequency.

Despite such high values, the impact on the RMS values is neglectable: the voltage and current RMS value variation is less than 0,05% and 2%, respectively. This means the phenomena might not be identified by usual RMS meters.

III. PQ ANALYZER CHARACTERISTICS

Regarding the procedures for the analysis of the voltages and currents spectral content, the first version of the standard IEC 1000-4-7 [16] in 1991 considered alternatives of analysis “in the frequency domain”, performed through analog processing, or analysis “in the time domain”, performed through digital signal processing such as decomposition algorithms (e.g., DFT or FFT) and digital filtering. Amendments and later versions [17] incorporated novel technologies. Since the 2002 version of IEC 61000-4-7, only the use of digital systems has been established. The distinct processes documented in certain standards regarding measuring specific PQ disturbances have been aggregated in the standard EN 61000-4-30 (2003) [18], which has consolidated procedures for digitized measurements with the technology of that time. The 2015 version is the current version of this standard, with an amendment published in 2021 [1].

According to [17], the PQA should include an anti-aliasing filter in the input circuit so that "frequencies outside the measuring range of the instrument shall be attenuated so as not to affect the results. The instrument may sample the input signal at a frequency much higher than the measuring range to obtain the appropriate attenuation. For example, the analyzed signal may have components exceeding 25 kHz, but only components up to 2 kHz are considered. An anti-aliasing low-pass filter, with a –3 dB frequency above the measuring range, shall be provided. The attenuation in the stop-band shall exceed 50 dB”.

Note that this is just a numerical example of a filter characteristic. There are no detailed project or performance specifications in the standard. On the other hand, modern meters, with sampling frequency in the tens of kHz range, tend to enable extended harmonic analysis, reaching the limit of the Nyquist frequency. In these cases, the anti-aliasing filter will certainly not have the cutoff frequency close to the traditional harmonic range (2 to 3 kHz) but will be within the limits of half the sampling frequency. There is another concern about the fact that these filters limit the transient measurement capabilities of the instrument. One of the solutions is to pass the signal samples through the anti-aliasing filter only for low-order harmonic analysis.

The standard [1] states that using the anti-aliasing filter is optional for Class-S analyzers, and many Class-A PQAs offer the option to display results with or without this filter.

Still, according to [16], any two instruments that comply with the requirements of Class I, classified as Class-A in [1], when connected to the same signals, shall produce matching results within the specified accuracy”.

According to [19], the PQA can be used:

• in the generation, transmission, and distribution of electricity, for example, in a distributed generator connection;

• at the interface point between the installation and the network;

• these instruments can also be used for other applications, e.g. inside commercial/industrial installations.

A. *EFFECTS OF HIGH-FREQUENCY SIGNALS IN DIGITAL PQA*

Digital processing of the PQAs starts by sampling the voltage and current. It is usual to sample at a rate of 2^n samples per one cycle of the fundamental frequency or an integer number of cycles. This specification allows the calculation of the signal spectrum through a Fast Fourier Transform (FFT) algorithm. Thus, it is common to find PQAs with sampling rates of 256, 512 samples/cycle, or 4096 samples in 200 ms (10 cycles of 50 Hz or 12 cycles of 60 Hz), which is equivalent to 20.48 kHz.

It is well known that PQA correctly identifies the harmonic spectrum only up to its highest identifiable frequency, half of its sampling frequency, i.e., the Nyquist frequency. For example, a usual entry-level PQA that obtains the harmonic spectrum from an FFT algorithm with 128 samples per cycle can, theoretically, measure correctly up to the 63rd harmonic.

Consider the sampled current contains an amplified component at the PEC’s switching frequency, f_o. If f_o is lower than the half of the PQA’s sampling frequency, f_s, then f_o is identified correctly, since $f_o \in \Omega_N = (-f_N, f_N)$, where the Nyquist frequency is $f_N = f_s/2$.

However, if f_o is higher than f_N, the FFT identifies non-existing frequencies due to the aliasing effect. Eq. (1) defines δ as the difference between f_o and f_s:

$$\delta = f_o - f_s, \qquad \delta \in \Omega_N \tag{1}$$

Assuming that the f_o component of the sampled current is sinusoidal, its respective sampled value, y_o, is:

$$\mathrm{y_o[k]} = \mathrm{A}\, sin(2\pi f_o k T_s) = \mathrm{A}\, sin(2\pi(\delta + f_s)kT_s) \tag{2}$$

$$= \mathrm{A}(sin(2\pi\delta kT_s)\, cos(2\pi f_s kT_s) + cos(2\pi\delta kT_s)\, sin(2\pi f_s kT_s)),$$

where A, $k \in \mathbb{N}$, and $T_s = 1/f_s$ correspond to the signal amplitude, the number of samples, and the sampling period, respectively. Since $cos(2\pi k f_s T_s) = 1$ and $sin(2\pi k f_s T_s) = 0$, the sampled signal becomes:

$$\mathrm{y_o[k]} = \mathrm{A}\, sin(2\pi\delta kT_s) \tag{3}$$

which shows that the frequency of the sampled f_o component is now δ.

Although the spectrum due to the PWM switching is much more complex than a single sinusoidal signal [19], the result in (3) is enough for the analysis in the next section.

From (3), it is logical to conclude that PQAs may provide misleading results depending on the high-frequency components of the measured signals. The next section shows, among other results, the case of a PQA that samples at 20.48 samples per second, or 4096 samples over 200 ms, and displays non-existing harmonics for measured signals with components around the 20-kHz frequency range in a 60-Hz grid.

IV. HARMONICS MEASUREMENT

A single-phase, 220 V PV inverter with a 20-kHz nominal PWM switching frequency was connected to a 60-Hz low-voltage microgrid [21]. In a near “consumer unit”, 25 m from the PCC of the PV inverter, a set of loads composed of LED lamps, one PC power supply, and RC passive loads was connected, totaling 500 VA. Analysis showed that the connection of the equivalent capacitance of the load set and the cabling inductance resulted in a series resonance of approximately 20 kHz, with similar waveforms as displayed in Figure 3. The total load RMS fundamental current is 2.25 A. The resonant component at 20 kHz varies along the 60-Hz cycle and, at the maximum situation, reaches 1.34 A (3.9 A peak-to-peak). All the instruments correctly indicate the fundamental current.

In this context, the spectral analysis was performed by installing three Class-A PQAs and an oscilloscope at the point of common coupling of the load set, according to the guidelines in [19].

It is important to emphasize that the anti-aliasing filter of the PQAs was active, which means the switching frequency present in the measured signal was attenuated before the sampling. However, the cut-off frequency of the respective anti-aliasing filters is unknown.

FIGURE 4. The experimental microgrid's measurement setup shows the PQAs, inverters, and additional instrumentation.

The sampling rate and the vertical resolution of the PQAs are in Table 1. The oscilloscope is used as a benchmark due to its highest sampling rate. The current probe has a resolution of 1 mA and a bandwidth of 100 kHz.

According to [15], the measurement procedure uses rectangular windowing. For the FFT procedure, the PQA1 processes 4096 samples per 200 ms, PQA2 processes 512 samples per cycle, and PQA3 uses 256 samples per cycle. Table 2 resumes the measured current THD (THDi) of each instrument.

TABLE 1. Measurement device characteristics.

Device	Sampling frequency	ADC resolution
PQA1	20.48 kHz	16 bits
PQA2	30.72 kHz	16 bits
PQA3	15.36 kHz	16 bits
Oscilloscope	5 MHz	10 bits

TABLE 2. THD of the measured current.

Device	TDHi up to 50^{th} harmonic	TDHi at full sampling range
PQA1	5 %	Not available
PQA2	1.6 %	36 %
PQA3	2.5 %	38 %
Oscilloscope	0.7 %	Not available

Figure 5 shows the harmonic histogram of the current at the PCC of the load set up to the 50^{th} harmonic from all devices. The fundamental component is omitted.

Similar results are observed on the PCC of the PV inverter, which was expected since the current circulates between the PCCs, as shown in Figure 6.

Even with the anti-aliasing filter active, the effect of the switching frequency component combined with the PQA1 sampling rate is evident. From (3), the sampled signal in PQA1 contains a spectral component around 480 Hz. Note in Figure 5 that the PQA1 overestimates the 5^{th} (300 Hz), 7^{th} (420 Hz), 9^{th} (520 Hz), and 11^{th} (660 Hz) harmonics, which is consistent with the actual scattering of the PWM spectrum.

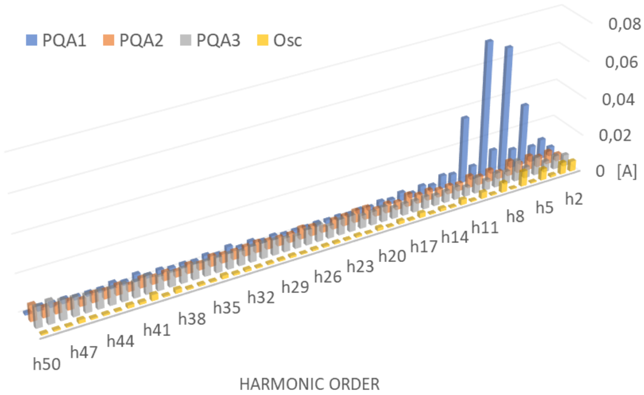

FIGURE 5. Harmonic spectrum of measured current with different PQ analyzers connected at the same PCC. The fundamental component is omitted.

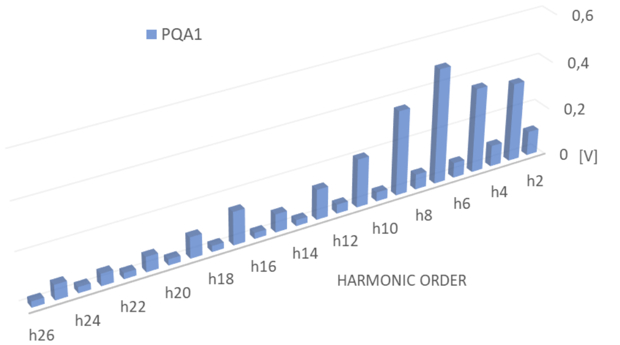

FIGURE 6. Harmonic spectrum of measured voltage with PQA1 analyzers connected at the PCC. The fundamental component is omitted.

PQA2 and PQA3 have similar results to the oscilloscope, which is also consistent with (3) considering only the 3-kHz range. Table 1 shows that the spurious harmonic components affect the THD value.

Limiting the harmonic order to 50, PQA2 and PQA3 do not include the high-frequency spectral components. Widing the range, such harmonics will drastically increase the THDi, as shown in Figure 7 and Figure 8. The THDi of PQA2 and PQA3 for the full sampling range, considered up to the 255^{th}

and 127th harmonic, respectively.

Note that, in the digital processing of PQAs, inter harmonics are grouped and counted in the nearest integer harmonic order [1].

Figure 7 shows the sampled current and the respective harmonic histogram at the full sampling range of PQA2. As the PV inverter operates at 20 kHz, from (3), the PWM switching frequency is erroneously identified at 10.72 kHz, indicating components around the 179th harmonic, or 10740 Hz.

Figure 8 shows the analogous results for PQA3. Similarly, non-existing harmonics are located around the 77th harmonic or 4620 Hz, corresponding to the difference between the real PEC switching frequency (20 kHz) and the PQA sampling frequency (15.36 kHz).

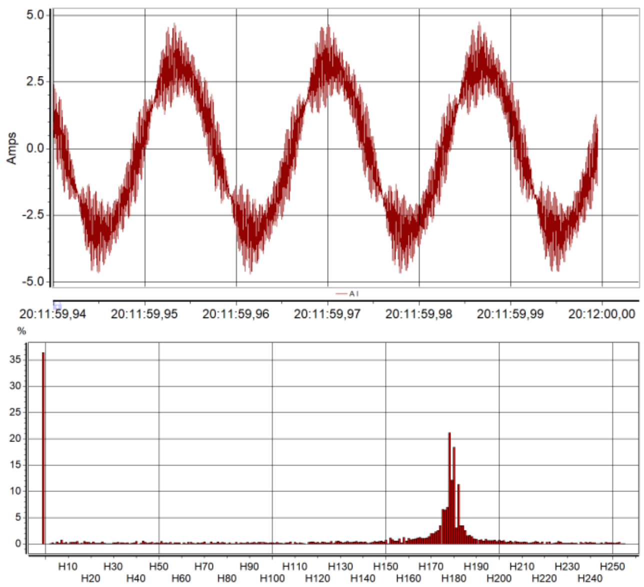

FIGURE 7. PQA2 harmonic spectrum at full sampling range and THDi (bar at foremost left-hand side). Sampling frequency: 30.72 kHz.

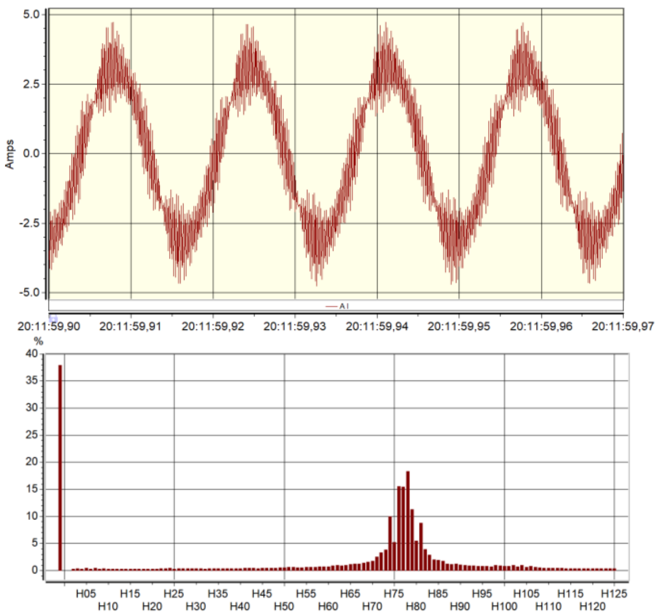

FIGURE 8. PQA3 harmonic spectrum at full sampling range and THDi (bar at foremost left-hand side). Sampling frequency: 15.36 kHz.

V. CONCLUSION

This paper presented the results of harmonic measurements from commercial PQAs installed in a grid with several PECs. The procedures comply with the specifications of the pertinent standards.

At first, it was shown that the interaction between the front-end elements of the internal PEC filters may create conditions for amplifying switching frequency spectral components in the current but also in the voltage.

It was demonstrated that these high-frequency components, when sampled by a PQA, may lead to incorrect identification of the harmonic spectrum and the THD value. If the high-frequency component is near the sampling frequency of the PQA, it will appear alias harmonics.

The classical solution is the use of an anti-aliasing filter. However, EN 61000-4-30 states that using an anti-aliasing filter is optional for Class-S analyzers, and many Class-A PQAs offer the option to sample with or without this filter. Anyway, even using the anti-aliasing filter, as shown in the experimental measurements, the PQA may present wrong results since the filter attenuation can be insufficient to cancel the switching frequency component.

Some PQA models allow the so-called “extended range” harmonic analysis, displaying the spectrum up to the Nyquist frequency. In this case, if used, the cut-off frequency anti-aliasing filter is allocated above half of the sampling frequency, providing low attenuation of the typical PEC switching frequency.

Even if the supra harmonic phenomena are not yet defined as a power quality problem, a wrong harmonic measurement is certainly a problem.

Standards seek to establish limits to normalize procedures but cannot foresight all new phenomena that can arise due to technological changes.

As shown in the studied case, the interaction among the filters of PECs, loads, and the electrical grid amplifies high-frequency spectral components produced by the PWM switching frequency embedded in modern PECs.

Until regulatory bodies define standard procedures for measuring and analyzing signals that may contain high-frequency spectral components, measurement campaigns in networks where relatively high-power power electronic converters (such as PV systems and EV chargers) exist or may exist should be carried out with some additional precautions.

As the PEC technologies are continuously changing, for example, substituting silicon for silicon carbide devices, the switching frequency tends to increase. Consequently, even modern PQAs with 100- or 200-kHz sampling frequency may present the same errors.

Considering that for a power distribution company, it is not feasible to make voltage and current measurements with an oscilloscope (high acquisition rate), procedures that can reduce the probability of obtaining harmonics erroneous measurements could be:

1) Identify whether the network to be analyzed has (or may have) medium to high-power PECs;

2) Use, at least initially, two PQAs with different (and known) sampling frequencies;

3) Record waveforms (snap-shots) at regular intervals (e.g., 15 minutes) for later spectral analysis;

4) In a preliminary short-term measurement (24 hours), compare the harmonic spectra of both PQAs;

5) Analyze the results of the limited spectrum (2 to 3 kHz) and the extended-spectrum in search of significant differences between the PQAs, which could indicate the occurrence of aliasing;

6) If the measurements are consistent, the standard one-week measurement procedure can be done using only one of the PQAs.

ACKNOWLEDGMENT

This work was supported in part by the São Paulo Research Foundation (FAPESP), grant #2016/08645-9, and by the Electricity Sector Research and Development Program PD-00063-3058/2019 - PA3058: “MERGE - Microgrids for Efficient, Reliable and Greener Energy”, regulated by the National Electricity Agency (ANEEL), Brazil, in partnership with CPFL Energia.

The authors wish to thank the MEIHAPER Ibero-American Network, of CYTED, for the co-financing of Dr. Emmanuel Sangoi stay at the Smart Grid Laboratory, LabREI-Unicamp.

AUTHOR CONTRIBUTION

ORTENZI, G.: Conceptualization, Data Curation, Formal Analysis, Investigation, Methodology, Writing – Review & Editing. **SANGOI, E.**: Conceptualization, Data Curation, Formal Analysis, Methodology, Project Administration, Resources, Software, Validation, Visualization, Writing – Review & Editing. **POMILIO, J.A.**: Conceptualization, Formal Analysis, Funding Acquisition, Methodology, Project Administration, Resources, Supervision, Visualization, Writing – Original Draft, Writing – Review & Editing. **OTA, J.I.Y.**: Conceptualization, Formal Analysis, Methodology, Software, Visualization, Writing – Review & Editing. **CARNEIRO, R.K.**: Conceptualization, Formal Analysis, Investigation, Methodology, Validation, Writing – Review & Editing.

PLAGIARISM POLICY

This article was submitted to the similarity system provided by Crossref and powered by iThenticate – Similarity Check.

REFERENCES

[1] IEC, Testing and measurement techniques. Power quality measurement methods, EN 61000-4-30:2015+A1, 2021.

[2] B. Lasseter, "Microgrids [distributed power generation]," 2001 IEEE Power Engineering Society Winter Meeting. Conference Proceedings (Cat. No.01CH37194), Columbus, OH, USA, 2001, pp. 146-149 vol.1, doi: 10.1109/PESW.2001.917020.

[3] IEEE, "IEEE Application Guide for IEEE Std 1547™-2018, IEEE Standard for Interconnection and Interoperability of Distributed Energy Resources with Associated Electric Power Systems Interfaces," in IEEE Std 1547.2-2023 (Revision of IEEE Std 1547.2-2008), pp.1-291, 20 May 2024, doi: 10.1109/IEEESTD.2024.10534228.

[4] IEEE, "IEEE Standard for Harmonic Control in Electric Power Systems," in IEEE Std 519-2022 (Revision of IEEE Std 519-2014) , vol., no., pp.1-31, 5 Aug. 2022, doi: 10.1109/IEEESTD.2022.9848440.

[5] IEC, Industrial, scientific and medical equipment. Radio-frequency disturbance characteristics. Limits and methods of measurement, EN 55011:2016+A2, 2021.

[6] T. M. Mendes, D. D. Ferreira, L. R. M. Silva, P. F. Ribeiro, J. Meyer and C. A. Duque, "PLL Based Method for Supraharmonics Emission Assessment," in IEEE Transactions on Power Delivery, vol. 37, no. 4, pp. 2610-2620, Aug. 2022, doi: 10.1109/TPWRD.2021.3112404.

[7] J. A. Pomilio, A. F. Hernandes, D. P. Damasceno, M. P. Dias, J. I. Y. Ota, G. Ortenzi, R. K. Carneiro, "High-Frequency Interactions Among Power Converters in Built-in dc Networks," 2023 IEEE International Conference on Electrical Systems for Aircraft, Railway, Ship Propulsion and Road Vehicles & International Transportation Electrification Conference (ESARS-ITEC), Venice, Italy, 2023, pp. 1-6, doi: 10.1109/ESARS-ITEC57127.2023.10114908.

[8] D. Darmawardana, S. Perera, D. Robinson, P. Ciufo, J. Meyer, M. Klatt, and U. Jayatunga, "Investigation of high frequency emissions (supraharmonics) from small, grid-tied, photovoltaic inverters of different topologies," 2018 18th International Conference on Harmonics and Quality of Power (ICHQP), Ljubljana, Slovenia, 2018, pp. 1-6, doi: 10.1109/ICHQP.2018.8378926.

[9] A. Grevener, J. Meyer, S. Rönnberg, M. Bollen, and J. Myrzik, “Survey of supraharmonic emission of household appliances,” CIRED – Open Access Proceedings Journal, vol. 2017, n. 1, pp. 870–874, 2017, doi: 10.1049/oap-cired.2017.0458.

[10] R. K. Carneiro, J. I. Y. Ota and J. A. Pomilio, "Field Measurements of Non-intentional Emissions above 2 kHz in Photovoltaic Inverter Installations," 2020 IEEE 29th International Symposium on Industrial Electronics (ISIE), Delft, Netherlands, 2020, pp. 1503-1508, doi: 10.1109/ISIE45063.2020.9152213.

[11] A. Hoevenaars, M. Farbis, M. McGraw, "Active Harmonic Mitigation: What the Manufacturers Don't Tell You," in *IEEE Industry Applications Magazine*, vol. 26, no. 5, pp. 41-51, Sept.-Oct. 2020, doi: 10.1109/MIAS.2020.2982484.

[12] Joint Working Group C4.24/CIRED, Power Quality and EMC Issues with Future Electricity Networks, CIGRE, Tech. Brochure 719, 2018.

[13] M. Bollen, M. Olofsson, A. Larsson, S. Rönnberg and M. Lundmark, "Standards for supraharmonics (2 to 150 kHz)," in IEEE Electromagnetic Compatibility Magazine, vol. 3, no. 1, pp. 114-119, 1st Quarter 2014, doi: 10.1109/MEMC.2014.6798813.

[14] G. Ortenzi and J. A. Pomilio, "Inside Residential Distributed Generation: A Look of High Frequency Contamination," 2021 Brazilian Power Electronics Conference (COBEP), João Pessoa, Brazil, 2021, pp. 1-6, doi: 10.1109/COBEP53665.2021.9684070.

[15] C. Nardi, C. M. O. Stein, E. G. Carati, J. P. Costa and R. Cardoso, "A methodology of LCL filter design for grid-tied power converters," 2015 IEEE 13th Brazilian Power Electronics Conference and 1st Southern Power Electronics Conference (COBEP/SPEC), Fortaleza, Brazil, 2015, pp. 1-5, doi: 10.1109/COBEP.2015.7420101.

[16] IEC, General guide on harmonics and interharmonics measurements and instrumentation, for power supply systems and equipment connected thereto, IEC 1000-4-7:1991.

[17] IEC, Testing and measurement techniques. General guide on harmonics and interharmonics measurements and instrumentation, for power supply systems and equipment connected thereto, EN 61000-4-7:2002+A1, 2009.

[18] IEC, Testing and measurement techniques. Power quality measurement methods, EN 61000-4-30:2003.

[19] IEC, Power quality measurement in power supply systems. Power quality instruments (PQI), EN 62586-1:2017, Nov. 2017.

[20] D. G. Holmes, T. A. Lipo, Pulse Width Modulation for Power Converters: Principles and Practice, Wiley-IEEE Press, 2003.

[21] J. A. Pomilio, J. I. Y. Ota, E. Sangoi, G. Ortenzi and R. K. Carneiro, "PQ Measurement Errors Due to High Frequency Distortion Produced by Power Electronics Converters," 2022 IEEE 7th Southern Power Electronics Conference (SPEC), Nadi, Fiji, 2022, pp. 1-5, doi: 10.1109/SPEC55080.2022.10058236.

BIOGRAPHIES

Gustavo Ortenzi was born in Campinas, Brazil, in 1977. He received a B.S. degree from the Federal University of Itajubá, Itajubá, Brazil, in 2002 and an M.S. degree from the University of Campinas, Campinas, Brazil, in 2009, both in electrical engineering. He acted as a hardware engineer for Whirlpool, Elsys, and Itron from 2002 to 2010, 2010 to 2011, and 2011 to 2014, respectively. From 2014 to 2022, he acted as a Senior Distribution Automation engineer in the Smart Grids department at Neoenergia Elektro, where he also acted as a researcher in R&D projects. He is currently acting as lead engineer for distribution automation at Avangrid-USA. His research interests include power electronics, microgrids, power quality, and EMC/EMI. Gustavo is a student member of the Brazilian Power Electronics Society. He has served as a reviewer for the COBEP 2009.

Emmanuel Sangoi was born in Santa Fe, Argentina, in 1986. He received a B. S. degree in electrical engineering and a D. degree in Industrial Engineering, both from Santa Fe Regional Faculty of National Technological University, Santa Fe, Argentina, in 2015 and 2021, respectively. From January 2018 to May 2018, he was a visiting student at the University of Ontario Institute of Technology, Ontario, Canada. Since February 2020, Dr. Sangoi has participated actively at the Research and Development Center in Electrical Engineering and Energy Systems (CIESE), and he is an assistant professor in the Department of Electrical Engineering, both activities at Santa Fe Regional Faculty of National Technological University. His research interests include power quality, solar photovoltaic energy, and smart grids.

José Antenor Pomilio was born in Jundiaí, Brazil, in 1960. He received his B.S., M.S., and Ph.D. in electrical engineering from the University of Campinas, Campinas, Brazil, in 1983, 1986, and 1991, respectively. From 1988 to 1991, he was the Head of the Power Electronics Group, Brazilian Synchrotron Light Laboratory. He was a visiting professor at the University of Padova in 1993 and 2015 and at the Third University of Rome in 2003 in Italy. He is a Professor at the School of Electrical and Computer Engineering, University of Campinas, where he has been teaching since 1984. His main interests are power electronics and power quality. Dr. Pomilio was the President of the Brazilian Power Electronics Society in 2000–2002 and a member of the Administrative Committee of the IEEE Power Electronics Society in 1997–2002.

João I. Y. Ota was born in São Paulo, Brazil, in 1985. He received the B.S. and M.S. degrees in electrical engineering from the University of Campinas, Campinas, Brazil, in 2009 and 2011, respectively, and the D. Eng. degree from Institute of Science Tokyo (formerly Tokyo Institute of Technology until Sept. 2024), Tokyo, Japan, in 2016. From 2018 to 2023, he was a Post-doctoral researcher at Smart Grid Lab (LabREI), University of Campinas. Since 2023, he has been a R&D Engineer at Hitachi Energy Sweden AB, Västerås, Sweden. His current research interests include low-voltage grid-connected power converters, such as battery energy storage systems and active harmonic filters, power converters applied to microgrids, and modular multilevel converters for STATCOMs and BESSs.

Rafael Kotchetkoff Carneiro, born on 09/29/1994 in São Paul, Brazil, is an electrical technician (2011), electrical engineer (2017), and master (est. 2024) in Electrical Engineer with the University of Campinas (UNICAMP). He is currently an invited professor at the University of Guyane, in French Guiana, as well as Technical Director of RKC Engenharia in Brazil and Solamaz in France. His areas of interest are power quality, photovoltaic generation, power electronics, microgrids, and electrical technical education for remote areas. Rafael is a member of the IEEE.